Structural factors impacting carrier transport and electroluminescence from Si nanocluster-sensitized Er ions

Sébastien Cueff,[1,4] Christophe Labbé,[1,*] Olivier Jambois,[2] Yonder Berencén,[2] Anthony J. Kenyon,[3] Blas Garrido,[2] and Richard Rizk[1]

[1]*Centre de Recherche sur les Ions, les Matériaux et la Photonique (CIMAP), ENSICAEN, CNRS, CEA/IRAMIS, Université de Caen, 14050 CAEN cedex, France*
[2]*Dept. Electrònica, MIND-IN2UB, Universitat de Barcelona, Martí i Fanquès 1, 08028 Barcelona, CAT, Spain*
[3]*Department of Electronic & Electrical Engineering, UCL, Torrington Place, London WC1E 7JE, UK*
[4]*Present address: Brown University, School of Engineering, Providence, Rhode Island 02912, USA*
[*]*christophe.labbe@ensicaen.fr*

Abstract: We present an analysis of factors influencing carrier transport and electroluminescence (EL) at 1.5 µm from erbium-doped silicon-rich silica (SiO_x) layers. The effects of both the active layer thickness and the Si-excess content on the electrical excitation of erbium are studied. We demonstrate that when the thickness is decreased from a few hundred to tens of nanometers the conductivity is greatly enhanced. Carrier transport is well described in all cases by a Poole-Frenkel mechanism, while the thickness-dependent current density suggests an evolution of both density and distribution of trapping states induced by Si nanoinclusions. We ascribe this observation to stress-induced effects prevailing in thin films, which inhibit the agglomeration of Si atoms, resulting in a high density of sub-nm Si inclusions that induce traps much shallower than those generated by Si nanoclusters (Si-ncs) formed in thicker films. There is no direct correlation between high conductivity and optimized EL intensity at 1.5 µm. Our results suggest that the main excitation mechanism governing the EL signal is impact excitation, which gradually becomes more efficient as film thickness increases, thanks to the increased segregation of Si-ncs, which in turn allows more efficient injection of hot electrons into the oxide matrix. Optimization of the EL signal is thus found to be a compromise between conductivity and both number and degree of segregation of Si-ncs, all of which are governed by a combination of excess Si content and sample thickness. This material study has strong implications for many electrically-driven devices using Si-ncs or Si-excess mediated EL.

OCIS codes: (160.5690) Rare-earth-doped materials; (130.0250) Optoelectronics; (220.4241) Nanostructure fabrication; (230.3670) Light-emitting diodes.

References and links

1. L. T. Canham, "Silicon quantum wire array fabrication by electrochemical and chemical dissolution of wafers," Appl. Phys. Lett. **57**(10), 1046–1048 (1990).
2. L. Pavesi, L. Dal Negro, C. Mazzoleni, G. Franzò, and F. Priolo, "Optical gain in silicon nanocrystals," Nature **408**(6811), 440–444 (2000).
3. J. Valenta, N. Lalic, and J. Linnros, "Electroluminescence of single silicon nanocrystals," Appl. Phys. Lett. **84**(9), 1459–1461 (2004).
4. G. Franzò, A. Irrera, E. C. Moreira, M. Miritello, F. Iacona, D. Sanfilippo, G. Di Stefano, P. G. Fallica, and F. Priolo, "Electroluminescence of silicon nanocrystals in MOS structures," Appl. Phys., A Mater. Sci. Process. **74**(1), 1–5 (2002).
5. D. Timmerman, I. Izeddin, P. Stallinga, I. N. Yassievich, and T. Gregorkiewicz, "Space-separated quantum cutting with silicon nanocrystals for photovoltaic applications," Nat. Photonics **2**(2), 105–109 (2008).

#167472 - $15.00 USD Received 27 Apr 2012; revised 6 Jul 2012; accepted 12 Jul 2012; published 17 Sep 2012

6. F. Sgrignuoli, G. Paternoster, A. Marconi, P. Ingenhoven, A. Anopchenko, G. Pucker, and L. Pavesi, "Modeling of silicon nanocrystals based down-shifter for enhanced silicon solar cell performance," J. Appl. Phys. **111**(3), 034303 (2012).
7. N. N. Ha, S. Cueff, K. Dohnalová, M. T. Trinh, C. Labbé, R. Rizk, I. N. Yassievich, and T. Gregorkiewicz, "Photon cutting for excitation of Er^{3+} ions in SiO_2 sensitized by Si quantum dots," Phys. Rev. B **84**(24), 241308 (2011).
8. R. J. Walters, P. G. Kik, J. D. Casperson, H. A. Atwater, R. Lindstedt, M. Giorgi, and G. Bourianoff, "Silicon optical nanocrystal memory," Appl. Phys. Lett. **85**(13), 2622–2624 (2004).
9. A. Mehonic, S. Cueff, M. Wojdak, S. Hudziak, O. Jambois, C. Labbé, B. Garrido, R. Rizk, and A. J. Kenyon, "Resistive switching in silicon suboxide films," J. Appl. Phys. **111**(7), 074507 (2012).
10. A. J. Kenyon, P. F. Trwoga, M. Federighi, and C. W. Pitt, "Optical properties of PECVD erbium-doped silicon-rich silica: evidence for energy transfer between silicon microclusters and erbium ions," J. Phys. Condens. Matter **6**(21), L319–L324 (1994).
11. S.-Y. Seo, M.-J. Kim, and J. Shin, "The Nd-nanocluster coupling strength and its effect in excitation/de-excitation of Nd^{3+} luminescence in Nd-doped silicon-rich silicon oxide," Appl. Phys. Lett. **83**(14), 2778–2780 (2003).
12. M. Fujii, M. Yoshida, Y. Kanzawa, S. Hayashi, and K. Yamamoto, "1.54 μm photoluminescence of Er^{3+} doped into SiO_2 films containing Si nanocrystals: evidence for energy transfer from Si nanocrystals to Er^{3+}," Appl. Phys. Lett. **71**(9), 1198–1200 (1997).
13. F. Iacona, D. Pacifici, A. Irrera, M. Miritello, G. Franzò, F. Priolo, D. Sanfilippo, G. Di Stefano, and P. G. Fallica, "Electroluminescence at 1.54 μm in Er-doped Si nanocluster-based devices," Appl. Phys. Lett. **81**(17), 3242–3244 (2002).
14. A. Marconi, A. Anopchenko, G. Pucker, and L. Pavesi, "Silicon nanocrystal light emitting device as a bidirectional optical transceiver," Semicond. Sci. Technol. **26**(9), 095019 (2011).
15. D. Pacifici, G. Franzò, F. Priolo, F. Iacona, and L. Dal Negro, "Modeling and perspectives of the Si nanocrystals–Er interaction for optical amplification," Phys. Rev. B **67**(24), 245301 (2003).
16. I. Izeddin, A. S. Moskalenko, I. N. Yassievich, M. Fujii, and T. Gregorkiewicz, "Nanosecond dynamics of the near-infrared photoluminescence of Er-doped SiO_2 sensitized with Si nanocrystals," Phys. Rev. Lett. **97**(20), 207401 (2006).
17. O. Savchyn, F. R. Ruhge, P. G. Kik, R. M. Todi, K. R. Coffey, H. Nukala, and H. Heinrich, "Luminescence-center-mediated excitation as the dominant Er sensitization mechanism in Er-doped silicon-rich SiO_2 films," Phys. Rev. B **76**(19), 195419 (2007).
18. B. Garrido, C. García, S.-Y. Seo, P. Pellegrino, D. Navarro-Urrios, N. Daldosso, L. Pavesi, F. Gourbilleau, and R. Rizk, "Excitable Er fraction and quenching phenomena in Er-doped SiO_2 layers containing Si nanoclusters," Phys. Rev. B **76**(24), 245308 (2007).
19. A. J. Kenyon, M. Wojdak, I. Ahmad, W. H. Loh, and C. J. Oton, "Generalized rate-equation analysis of excitation exchange between silicon nanoclusters and erbium ions," Phys. Rev. B **77**(3), 035318 (2008).
20. J. H. Shin, J. Lee, H.-S. Han, J.-H. Jhe, J. S. Chang, S.-Y. Seo, H. Lee, and N. Park, "Si nanocluster sensitization of Er-doped silica for optical amplet using top-pumping visible LEDs," IEEE J. Sel. Top. Quantum Electron. **12**(4), 783–796 (2006).
21. F. Priolo, C. D. Presti, G. Franzò, A. Irrera, I. Crupi, F. Iacona, G. Di Stefano, A. Piana, D. Sanfilippo, and P. G. Fallica, "Carrier-induced quenching processes on the erbium luminescence in silicon nanocluster devices," Phys. Rev. B **73**(11), 113302 (2006).
22. O. Jambois, Y. Berencen, K. Hijazi, M. Wojdak, A. J. Kenyon, F. Gourbilleau, R. Rizk, and B. Garrido, "Current transport and electroluminescence mechanisms in thin SiO_2 films containing Si nanocluster-sensitized erbium ions," J. Appl. Phys. **106**(6), 063526 (2009).
23. A. Anopchenko, A. Tengattini, A. Marconi, N. Prtljaga, J. M. Ramirez, O. Jambois, Y. Berencen, D. Navarro-Urrios, B. Garrido, F. Milesi, J. P. Colonna, J. M. Fedeli, and L. Pavesi, "Bipolar pulsed excitation of erbium-doped nanosilicon light emitting diodes," J. Appl. Phys. **111**(6), 063102 (2012).
24. J. M. Ramírez, F. Ferrarese Lupi, O. Jambois, Y. Berencén, D. Navarro-Urrios, A. Anopchenko, A. Marconi, N. Prtljaga, A. Tengattini, L. Pavesi, J. P. Colonna, J. M. Fedeli, and B. Garrido, "Erbium emission in MOS light emitting devices: from energy transfer to direct impact excitation," Nanotechnology **23**(12), 125203 (2012).
25. O. Jambois, F. Gourbilleau, A. J. Kenyon, J. Montserrat, R. Rizk, and B. Garrido, "Towards population inversion of electrically pumped Er ions sensitized by Si nanoclusters," Opt. Express **18**(3), 2230–2235 (2010).
26. G. M. Miller, R. M. Briggs, and H. A. Atwater, "Achieving optical gain in waveguide-confined nanocluster-sensitized erbium by pulsed excitation," J. Appl. Phys. **108**(6), 063109 (2010).
27. H. Jayatilleka, A. Nasrollahy-Shiraz, and A. J. Kenyon, "Electrically pumped silicon waveguide light sources," Opt. Express **19**(24), 24569–24576 (2011).
28. S. Cueff, C. Labbé, O. Jambois, B. Garrido, X. Portier, and R. Rizk, "Thickness-dependent optimization of Er^{3+} light emission from silicon-rich silicon oxide thin films," Nanoscale Res. Lett. **6**(1), 395 (2011).
29. S. Cueff, C. Labbé, J. Cardin, J.-L. Doualan, L. Khomenkova, K. Hijazi, O. Jambois, B. Garrido, and R. Rizk, "Efficient energy transfer from Si-nanoclusters to Er ions in silica induced by substrate heating during deposition," J. Appl. Phys. **108**(6), 064302 (2010).
30. J. Frenkel, "On the theory of electrical breakdown of dielectrics and electronic semiconductors," Tech. Phys. USSR **5**, 685–687 (1938).

#167472 - $15.00 USD Received 27 Apr 2012; revised 6 Jul 2012; accepted 12 Jul 2012; published 17 Sep 2012

31. S. Cueff, C. Labbé, B. Dierre, J. Cardin, L. Khomenkova, F. Fabbri, T. Sekiguchi, and R. Rizk, "Cathodoluminescence and photoluminescence comparative study of erbium-doped silicon-rich silicon oxide," J. Nanophotonics **5**(1), 051504 (2011).
32. S. Cueff, C. Labbé, K. Watanabe, B. Dierre, T. Sekiguchi, and R. Rizk, "Nature and role of various Si-based sensitizers for Er^{3+} ions in silicon-rich silicon oxide thin films," Adv. Mat. Res. **324**, 81–84 (2011).
33. T. Z. Lu, M. Alexe, R. Scholz, V. Talalaev, R. J. Zhang, and M. Zacharias, "Si nanocrystal based memories: effect of the nanocrystal density," J. Appl. Phys. **100**(1), 014310 (2006).
34. J. G. Simmons, "Poole-Frenkel effect and Schottky effect in metal-insulator-metal systems," Phys. Rev. **155**(3), 657–660 (1967).
35. A. Marconi, A. Anopchenko, M. Wang, G. Pucker, P. Bellutti, and L. Pavesi, "High power efficiency in Si-nc/SiO_2 multilayer light emitting devices by bipolar direct tunneling," Appl. Phys. Lett. **94**(22), 221110 (2009).
36. Z. Yuan, G. Pucker, A. Marconi, F. Sgrignuoli, A. Anopchenko, Y. Jestin, L. Ferrario, P. Bellutti, and L. Pavesi, "Silicon nanocrystals as a photoluminescence down shifter for solar cells," Sol. Energy Mater. Sol. Cells **95**(4), 1224–1227 (2011).
37. A. Anopchenko, A. Marconi, M. Wang, G. Pucker, P. Bellutti, and L. Pavesi, "Graded-size Si quantum dot ensembles for efficient light-emitting diodes," Appl. Phys. Lett. **99**(18), 181108 (2011).
38. O. Jambois, J. M. Ramírez, Y. Berencén, D. Navarro-Urrios, A. Anopchenko, A. Marconi, N. Prtljaga, A. Tengattini, P. Pellegrino, N. Daldosso, L. Pavesi, J.-P. Colonna, J.-M. Fedeli, and B. Garrido, "Effect of the annealing treatments on the electroluminescence efficiency of SiO2 layers doped with Si and Er," J. Phys. D Appl. Phys. **45**(4), 045103 (2012).
39. A. Anopchenko, A. Marconi, E. Moser, S. Prezioso, M. Wang, L. Pavesi, G. Pucker, and P. Bellutti, "Low voltage onset of electroluminescence in nanocrystalline-Si/ SiO_2 multilayers," J. Appl. Phys. **106**(3), 033104 (2009).
40. S. Habermehl and R. T. Apodaca, "Dielectric breakdown and Poole-Frenkel field saturation in silicon oxynitride thin films," Appl. Phys. Lett. **86**(7), 072103 (2005).
41. S. Savchyn, K. R. Coffey, and P. G. Kik, "Determination of optimum Si excess concentration in Er-doped Si-rich SiO_2 for optical amplification at 1.54 μm," Appl. Phys. Lett. **97**(20), 201107 (2010).
42. F. Gourbilleau, R. Madelon, C. Dufour, and R. Rizk, "Fabrication and optical properties of Er-doped multilayers Si-rich SiO_2/SiO_2: size control, optimum Er –Si coupling and interaction distance monitoring," Opt. Mater. **27**(5), 868–875 (2005).
43. H. Krzyżanowska, K. S. Ni, Y. Fu, and P. M. Fauchet, "Electroluminescence from Er-doped SiO_2/nc-Si multilayers under lateral carrier injection," Mater. Sci. Eng. B. In press.

1. Introduction

Owing to its exceptional properties, combined to abundance on Earth, silicon is naturally widely used in numerous man-made structures and devices. Its preeminence in the microelectronic industry, along with its poor optical properties resulting from its indirect band gap, restricted it for a while to being primarily an "electronic" material. However, seminal work from Canham on luminescent porous silicon [1] shook the general belief that silicon is not the appropriate choice for photonic applications. Since then, nanostructured silicon has emerged as a credible optoelectronic material showing a wealth of promising applications. Among the highlights of the field can be counted the observation of optical gain [2], as well as electroluminescence [3,4], from silicon nanocrystals both being important steps toward the fabrication of an electrically-driven silicon laser. Quantum-cutting using Si-ncs [5], Si-multilayer [6] or Si-ncs sensitized erbium [7] also holds promise for increasing the efficiency of current photovoltaic solar cells. Finally, optical memory effects in silicon nanocrystals have also been reported [8], and more recently memristive effects have been demonstrated [9], paving the way to realize an all silicon memristor. In addition, Si-ncs have also been shown to be efficient sensitizers for light-emitters such as rare-earth ions (erbium, neodymium,..) [10,11]. In these systems, Si-ncs act as antennas that increase by ~10^4 the effective absorption cross-section of the emitter under optical or electrical excitation [10,12,13]. Gathering all these discoveries, one can easily envision a fully Si-based micro-optoelectronic circuit in which logic and memory operations are operated by Si-based memristors and/or transistors, light is emitted and detected by Si-ncs based devices [14], and guided and amplified in Si-based waveguides. Such 'all-silicon' optical circuitry would be compatible for full integration on conventional CMOS chips at a low effective cost.

This picture is as yet far from being a reality, and many optimization steps are needed. Most of these Si-nc-based devices require (i) fine control of the Si-ncs size, structure and

#167472 - $15.00 USD Received 27 Apr 2012; revised 6 Jul 2012; accepted 12 Jul 2012; published 17 Sep 2012

separation over the whole active layer (ii) a better understanding of what governs the electrical transport of carriers and (iii) scalability to fit in nanometer-scale devices. Concerning potential CMOS-compatible electrically-driven photonic sources, SiO_x:Er could be implemented as optical interconnects operating at telecommunication wavelength (1.5 μm). Numerous excellent works on SiO_x:Er exist in the literature, but they are, in most cases, based on photoluminescence results [15–20]. The few reports of electroluminescence from SiO_x:Er demonstrate that Si excess in SiO_2 is absolutely needed to i) enhance the electrical conduction and injection of carriers and ii) allow efficient excitation of Er^{3+} ions [21,22]. Recent promising results were obtained under alternative current excitation scheme [23,24]. However, no net optical gain has yet been reported for electrically-driven SiO_x:Er devices, and the state-of-the-art highest fraction of electrically excited Er^{3+} ions is 20% [25]. Nevertheless, two recent simulation works showed that (i) it is theoretically possible to achieve modal gain via pulsed electrical excitation of waveguide-confined devices [26], and (ii) light can be efficiently coupled from electrically-pumped SiO_x:Er into silicon waveguides [27]. Such results are promising for future all-silicon optical-circuitry and highlight the need to better understand the physics of carrier transport and erbium excitation in fabricated devices.

In this paper we investigate the thickness-dependence of electrical transport of carriers and emission from nanocluster-sensitized erbium by means of studies of electrically-driven LEDs. Emphasis is first put on the Si-nc-assisted injection of carriers and material conduction properties. We demonstrate that the thickness of the active layer affects the structural properties of Si-ncs, altering the efficiency of carrier transport without significantly modifying the underlying physical mechanism (Poole-Frenkel). Our study probes the electrical effects of thickness-induced structural modifications of Si-ncs, due to film stress, and gives microscopic details of the transport of carriers between Si excess-based nanostructures. In a second strand, the sensitization of Er^{3+} by Si-ncs is investigated, again as a function of thickness and Si excess, to gain more insight into both the interplay between conductivity and Er emission, and the excitation mechanism of Er in this system. We show that when active layer thickness is reduced from hundreds to tens of nanometers, the normalized Er^{3+} emission signal per unit thickness is strongly reduced, although the conductivity is enhanced and the threshold voltage is lowered. This latter statement demonstrates that the Er^{3+} excitation is not directly correlated to the conductivity. Based on this work on LEDs, our conclusions can be applied to all kinds of electrically-driven devices (transistors, photovoltaics, nanocluster memories…) based on Si-ncs that require device dimensions of a few tens of nanometers.

2. Device processing and electrical characteristics

All LED devices were defined by photolithographically-etched SiO_2, delimiting a square-shaped through the sputtered active SiO_x:Er layers of various thicknesses to the p-type (100) Si substrate. The composition of the active layer was found to be unchanged when the film thickness was varied; further details of the deposition, as well as structural and compositional investigations, can be found elsewhere [28]. The deposition temperature was maintained at 500°C, corresponding to the optimum luminescent properties determined in a previous study [29]. A thin layer of Indium Tin Oxide (ITO) was then deposited on the whole surface and aluminum contacts were deposited as empty-square shapes to allow the emitted light to be transmitted through the top of the device (Fig. 1). All samples were annealed at 900°C in pure N_2 for 1h.

#167472 - $15.00 USD Received 27 Apr 2012; revised 6 Jul 2012; accepted 12 Jul 2012; published 17 Sep 2012

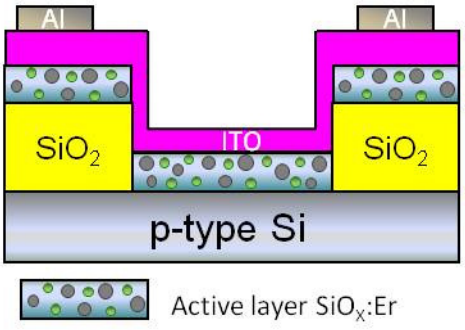

Fig. 1. Schematic cross-section view of the light emitting diode with an SiO_x:Er active layer analyzed in this work.

We first examine the electrical characteristics of LEDs for different thicknesses of the active layer, ranging from 20 nm to 170 nm. We measured the variation of the current density (J) as a function of the applied voltage (V) for each active layer thickness (d_{al}), as displayed in Fig. 2(a). An important parameter for device applications is the threshold voltage (V_{th}), which needs to be as low as a few volts to be integrated in existing CMOS devices. V_{th} is arbitrarily defined here as the voltage required for deflecting the I-V curve, thus allowing a significant current to start flowing through the active layer. V_{th} monotonically increases with the thickness with values ranging from 5 V (20 nm) to 25 V (170 nm).

LEDs comprising a sub-oxide thin film as an active layer often exhibit Poole-Frenkel (PF) conductivity when submitted to an external electric field. Electrons trapped in localized states have a probability to be thermally promoted to the conduction band. When an external electric field is applied, the potential barrier is lowered and the emission probability is greatly enhanced. This electric-field enhanced thermionic emission is described by the following relation between the current density and the applied voltage [30]:

$$J \propto \frac{V}{d_{al}} \cdot \exp\left(\frac{1}{k_B T} \left[\sqrt{\frac{e^3 V}{\pi \varepsilon_r \varepsilon_0 d_{al}}} \right] \right) \tag{1}$$

where k_B is Boltzmann's constant, T is the temperature (K), e is the electron charge, ε_r and ε_o respectively stand for the relative and vacuum permittivity. Equation (1) can straightforwardly be rearranged to:

$$\ln\left(\frac{J}{E}\right) \propto \left[\frac{1}{k_B T} \cdot \sqrt{\frac{e^3}{\pi \varepsilon_r \varepsilon_0}} \right] \cdot E^{1/2} \tag{2}$$

where $E = V/d_{al}$ stands for the electric field. Following Eq. (2), any LED displaying PF conduction would show a linear behavior if $\ln(J/E)$ is plotted as a function of $E^{1/2}$. The inset of Fig. 2(a) displays this PF representation for the thinnest and thickest layers studied (20 nm and 170 nm, respectively) as well as their corresponding fits using Eq. (2).

We find that all fabricated devices are well described by a PF conduction mechanism, similar to an earlier study on similar samples [22]. The dynamic permittivity ε_r, used here as a free fit parameter, is shown to be $\varepsilon_r = 3.0 \pm 0.2$ for all layers, indicating that there is no significant change in the composition when the thickness is increased. Such a result is consistent with our previous analysis of the composition profiles as a function of thickness [28]. We also report in Fig. 2(b) the values of the maximum voltage reached before

#167472 - $15.00 USD Received 27 Apr 2012; revised 6 Jul 2012; accepted 12 Jul 2012; published 17 Sep 2012

breakdown (V_{max}) against the thickness and the corresponding values of maximum current density reached before breakdown ($J_{max\ exp}$).

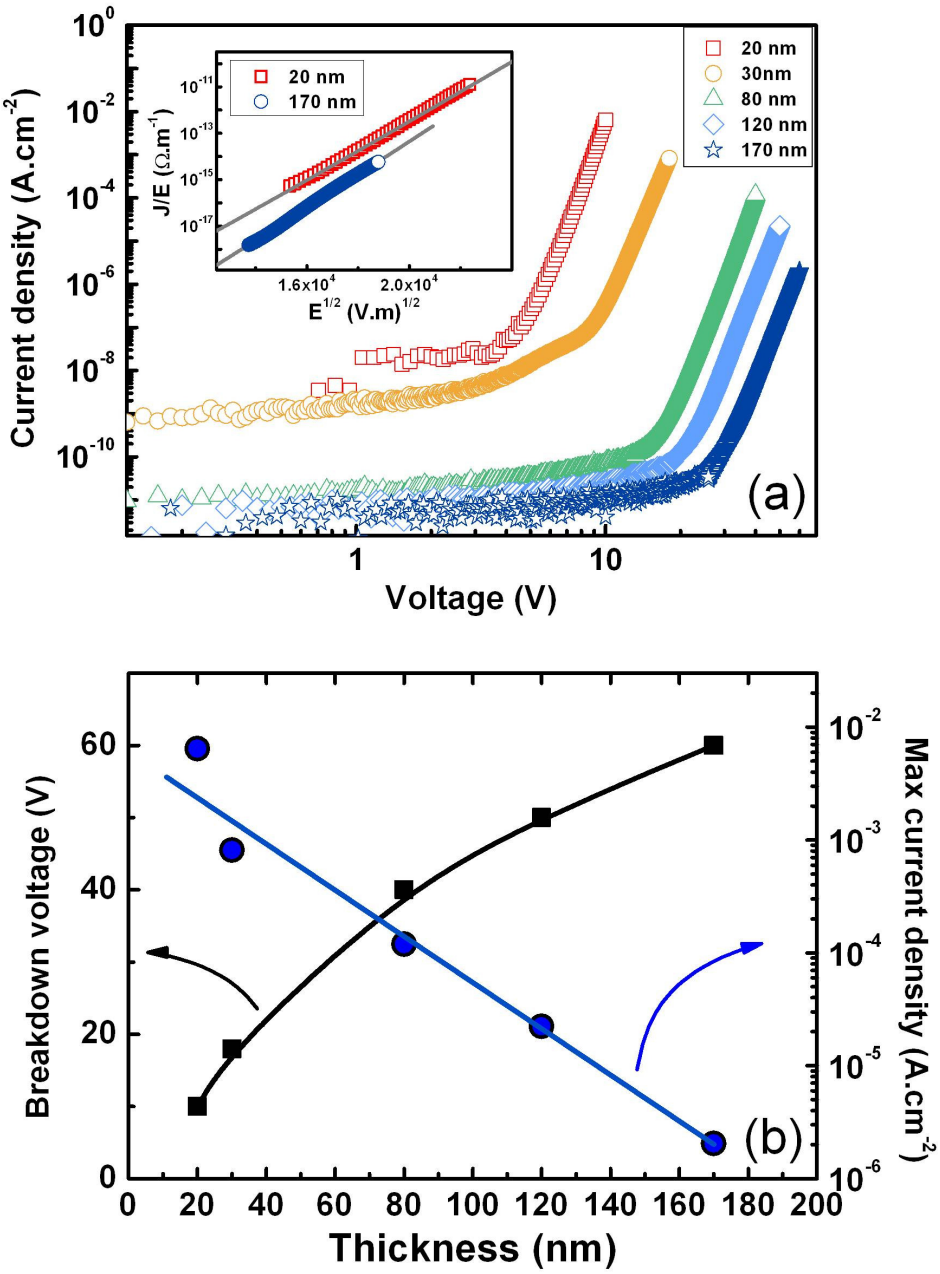

Fig. 2. (a) Current density versus applied voltage for SiO_x:Er layers of different thicknesses, ranging from 20 nm to 170 nm. Inset: Poole-Frenkel representation of conduction for layers of 20 nm and 170 nm. (b) Values of breakdown voltage and the corresponding maximum current density as a function of thickness.

Analysis of Figs. 2(a) and 2(b) suggests that thickness has a triple influence on the electrical properties of these layers through modification of three parameters: J, V_{th} and V_{max}.

#167472 - $15.00 USD Received 27 Apr 2012; revised 6 Jul 2012; accepted 12 Jul 2012; published 17 Sep 2012

However, the conduction mechanism is still unchanged, and is well described by the PF model for all values of thickness. Interestingly, the thinnest samples present the double advantage of showing both high J and low V_{th} and appear, at this stage, as the most suitable for highly efficient LEDs. As the same composition and the same transport mechanism prevail in all samples, the observed thickness-dependence of J and V_{th} somehow result either from the thickness itself or from a thickness-dependent arrangement of atoms inside the layer [28]. To investigate the likelihood of one or the other phenomenon, we use the relation describing the variation of J vs. d_{al} in PF mechanism (Eq. (1)).

Using the measured values of V_{max} and the corresponding thickness value d_{al}, Eq. (1) allows us to calculate the expected current density, J_{calc}. Figure 3 compares the thickness evolution of $J_{max\ calc}$ to that of the measured current density ($J_{max\ exp}$) shown in Fig. 2(b). Note that Eq. (1) does not allow the calculation of exact and absolute values. So, for the sake of comparison and a clear identification of the influence of the thickness on the current variation, we have normalized $J_{max\ calc}$ to J_0, defined as the $J_{max\ exp}$ value for the thickest sample at 170 nm, for which the stress (or thinness-limiting effects) can be considered to be negligible.

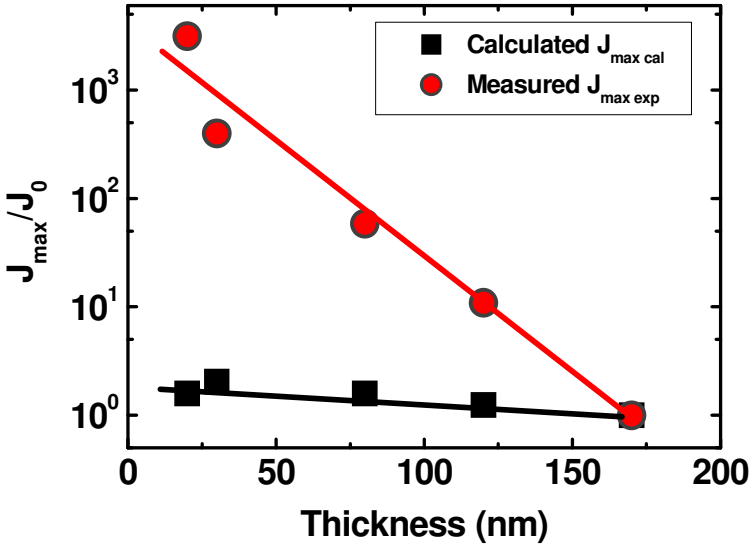

Fig. 3. Comparative evolutions of experimental and calculated values of the maximal current density flowing through active layers of LEDs of different thicknesses.

As depicted in Fig. 3, both $J_{max\ calc}$ and $J_{max\ exp}$ increase when the thickness is reduced. However, while $J_{max\ exp}$ rises by 4 orders of magnitude when the thickness is decreased from 170 nm to 20 nm, $J_{max\ calc}$ increases by less than one order of magnitude. According to this calculation the thickness decrease cannot explain itself the 4-order increase of current density. Consequently, this thickness dependence of $J_{max\ exp}$ is more likely to be the result of a change in the atomic arrangement within the active layers [28].

Previously, we showed that the compressive stress prevailing in films thinner than ~100 nm inhibits the agglomeration of excess Si atoms. Furthermore, this effect is inversely proportional to film thickness. Hence, for a given Si excess and thermal treatment, a 'thin' film (<100-150 nm) contains a high number of dispersed Si atoms that are preferentially arranged as defects (Silicon Oxygen-Deficient Centers - SiODC or Non-Bridging Oxygen Hole Centers - NBOHC) or very small agglomerates [28,31,32]. On the other hand, the same amount of Si excess in a 'thick' film (>100-150 nm) subject to the same heat treatment would

#167472 - $15.00 USD Received 27 Apr 2012; revised 6 Jul 2012; accepted 12 Jul 2012; published 17 Sep 2012

preferentially agglomerate in well-defined Si-ncs [28,31,32]. In thin films, this leads to a high number of structural defects and isolated atoms scattered throughout the layer, creating a high density of energy states close to the band edges. Such a quasi 'continuum' of shallow traps acting as relays for current transport [33] would enhance significantly the injection of carriers and lower the activation energy characterizing the thermal emission in the PF conduction mechanism . For thick films, in contrast, discrete Si-ncs are formed. Carriers are more deeply trapped in this case, requiring higher activation energy to hop from one Si-nc to another. The model suggested for each process is schematically illustrated in Fig. 4.

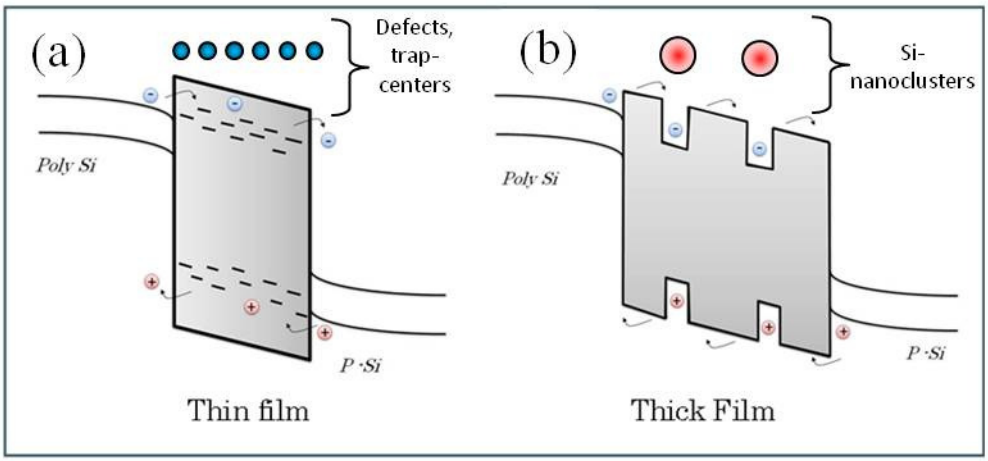

Fig. 4. Schematic model explaining the different conduction properties between (a) thin films (<150 nm) and (b) thick films (>150 nm). Interface defects are likely to be present in both kinds of samples but are not displayed here for clarity.

We note that this model is consistent with the measured progressive increase in the threshold voltage (Fig. 2(a)) as a function of thickness. V_{th} represents the minimum voltage needed to promote de-trapping of electrons, being linked to the charge trap potential depth. Thus, a low (high) V_{th} value indicates a shallow (deep) potential barrier that electrons must overcome to reach the conduction band. This phenomenon is consistent with the independently measured progressive agglomeration of Si excess with increasing film thickness [28], resulting in larger Si-ncs with higher potential energy barriers relative to the surrounding dielectric (SiO_2). The increasing value of V_{th} can thus be seen as a result of the increasing size of Si-ncs, which induce deeper and deeper trap states.

On the other hand, to test our assumption that there is a higher number of traps in thin films, one can analyze the so-called *low field conductivity* [34] (current before threshold) which is a direct indication of the charge trap density [33]. The observed progressive two-order of magnitude lowering of $J_{low\text{-}field}$ (Fig. 2(a)) with increasing thickness confirms a corresponding reduction in the number of traps.

These two kinds of conduction behavior are therefore due to the difference of excess Si agglomeration when the thickness is changed, which results in a four order of magnitude conduction difference between thinnest and thickest films. Put another way: both the number and the structure of Si-ncs are altered by the thickness of active layer. Such a phenomenon is reported for the first time here and reveals the interplay between thickness of active layer, microscopic structure of Si-ncs and electrical conduction properties. These latter results will undoubtedly have an impact on the previously mentioned applications of Si-ncs, notably on photovoltaics and electrically-driven devices such as memristors or LEDs. This may also have some repercussions on the design and nano-engineering on multiple monolayers of Si-ncs in SiO_2 [35], photoluminescence down shifter for solar cells [36] or graded-size Si

#167472 - $15.00 USD Received 27 Apr 2012; revised 6 Jul 2012; accepted 12 Jul 2012; published 17 Sep 2012

quantum dots [37]. We chose here to investigate further this thickness-dependence on the sensitization of Er^{3+} ions in such layers, which may lead to more insights on the excitation mechanism of these latter.

3. Conductivity-electroluminescence correlation

In Fig. 5, we report the variation of the EL signal at a wavelength of 1.5 µm as a function of the applied voltage for the indicated thicknesses. All layers contain 7 at.% excess Si. The erbium photoluminescence of similar SiO_x:Er samples (with thicknesses ranging from 15 nm to 170 nm), pumped through Si-ncs (λ_{ex} = 476 nm) is displayed in the upper inset, with the conductivities (σ = J/E) of corresponding LEDs displayed in the lower inset as a function of thickness.

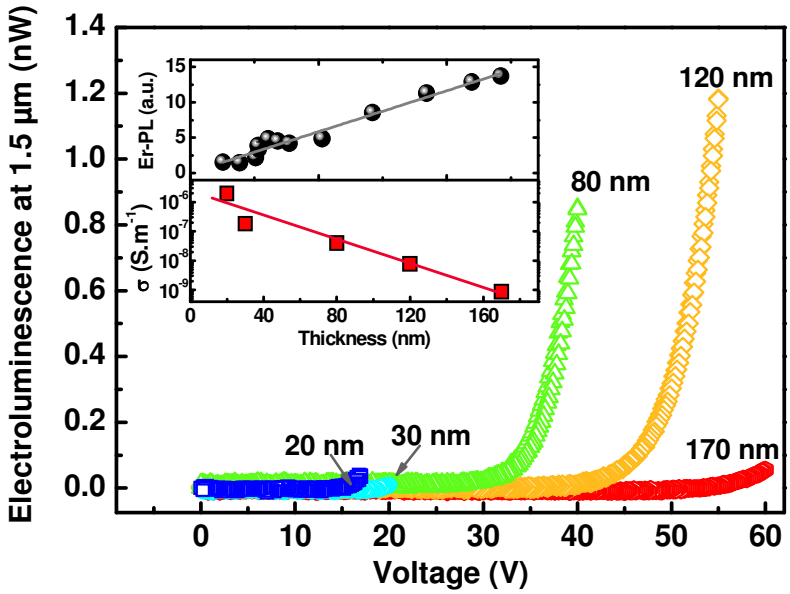

Fig. 5. EL versus applied voltage for different thicknesses of SiO_x:Er LEDs containing 7 at.% excess Si. Inset: relative evolution of Si-ncs sensitized Er PL at 1.5 µm and the conductivity for the same range of thicknesses.

The EL signal increases with the thickness, reaches an optimum at 120 nm and then strongly decreases for thicker layers (170 nm). As expected, EL at 1.5 µm begins when the current starts to flow through the active layer. But on the other hand, and counter-intuitively, the optimum thickness for electroluminescence (120 nm) does not correspond to the thickness of highest conductivity (20 nm). The optimum excitation of Er^{3+} ions is thus not only a matter of high density of current flowing through the SiO_x:Er layer. There is therefore no direct correlation between highest conductivity and optimum EL, unlike what is usually thought. In order to understand this paradox, the results displayed in the inset of Fig. 5 are helpful. The upper plot depicts the 1.5 µm photoluminescence intensity of Er^{3+} in SiO_x when pumped through Si-ncs, i.e. with a non-resonant wavelength (476 nm), normalized to both the thickness and the Er concentration. It shows a clear gradual and systematic increase of the Er^{3+} PL emission when thickness is increased from ~15 nm to ~170 nm. This phenomenon is due to a combination of inhibited formation of Si-based sensitizers and thickness-related optical effects (interferences, changes to the local density of optical states) [28]. The second plot in the inset shows that the conductivity is reduced in the meantime by almost four orders

#167472 - $15.00 USD Received 27 Apr 2012; revised 6 Jul 2012; accepted 12 Jul 2012; published 17 Sep 2012

of magnitude over the same thickness range. We can thus see that the EL signal at 1.5 µm is a difficult compromise between a good formation of Si-ncs to efficiently sensitize the Er^{3+} ions and a sufficiently high conductivity and low onset voltage to allow current to flow through the device. Note that these latter results are not sufficient to unambiguously draw conclusions about the physical mechanism governing the excitation of Er^{3+} ions. Recent studies, however, tend to show that impact excitation is the dominant excitation mechanism of Er^{3+} ions in SiO_x [24,38]. In this view, one can consider that the formation of larger Si-ncs in thick films (i.e. deep traps), would favor the creation of relatively hot electrons between clusters, producing Er^{3+} emission by impact excitation. On the other hand, in the case of a much more homogeneous distribution, the trap depth is too small to generate hot electrons, and hence Er^{3+} excitation (and emission) is correspondingly feeble. Note that, between these two extremes, the *number* of Si-ncs gradually changes. Thus, EL maximization is found when an appropriate balance is reached between a significant number of sensitizers (Si-ncs) and a sufficient trap-depth to produce hot electrons. This optimization is reached here at 120 nm.

A further interesting observation is that the EL signal is dramatically reduced for the 170 nm thick film. For this thickness, the onset voltage is very high (>50 V). Such high voltages, favors the injection of high-energy hot electrons [39,40], which is known to induce dielectric breakdown.

4. Trade-off between sample thickness and Si excess to optimize devices

In the previously mentioned simulation by Miller *et al.* [26], a 10 nm Er:Si-ncs layer (in SiO_2) slot waveguide sandwiched between two Si layers is proposed to obtain modal gain under a pulsed injection scheme. The study shows that modal gain can be enhanced from <1 dB/cm to 2-3 dB/cm when the thickness of active layer is increased from 10 nm to 50 nm. However, the thickness dependence is not taken into account in this simulation work, which may lead to significant deviation from the obtained simulation results. As pointed out in the introduction, any targeted application is likely to require a specific thickness (and geometry) of active layer for integration purposes. To reach this objective, one has to overcome the thickness-induced effects that result in the weak EL signals recorded in the few tens-of-nm-thick films. As previously explained, the low Er^{3+} emission in such thin films is mainly due to the limited number of large Si-ncs sensitizers (i.e. sufficient trap-depth to produce hot electrons) because of the thickness-induced inhibition of Si-ncs formation. To enhance the density of sensitizers in thin films, a simple solution is to increase the Si excess leading to the formation of more Si-ncs [28]. To study this, a set of samples with a Si excess of 18 at.% was tested. The EL signal was recorded as function of applied voltage for films with thicknesses between 15nm and 95nm (Fig. 6). The optimum EL signal is reached for ~40nm thick sample, with intensity twice as high as that for a similar thickness film with 7 at.% of Si excess. Such a shift of the optimum EL towards low thicknesses supports our assertion concerning the lack of sensitizers for Er^{3+} in thin films: when the Si excess is increased, the EL intensity is enhanced through a higher number of Si-ncs. Furthermore, it also demonstrates that device and sample optimization must properly take into account the active layer thickness. Existing literature reports on the determination of optimum Si excess for SiO_x:Er are therefore only valid for the thickness used by the authors (~110 nm) [41].

#167472 - $15.00 USD Received 27 Apr 2012; revised 6 Jul 2012; accepted 12 Jul 2012; published 17 Sep 2012

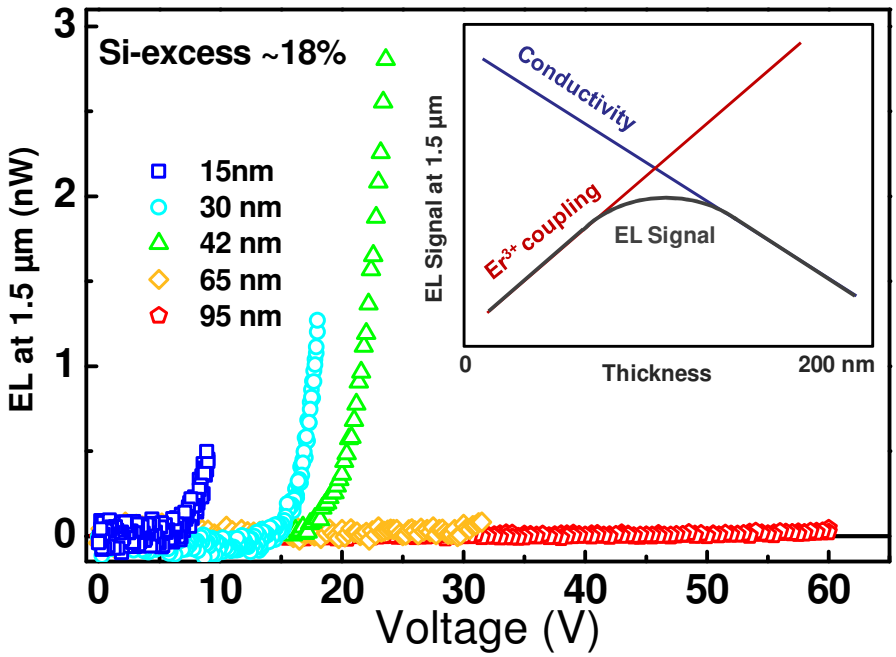

Fig. 6. Electroluminescence signal at 1.5 µm (normalized to film thickness) versus applied voltage for different thicknesses of SiO_x:Er layers containing 18 at.% Si-excess. Inset: scheme of the combined influences of conductivity and Er^{3+} coupling on the resulting EL signal.

Note that the conductivity for these high Si excess layers also shows a four order of magnitude decrease when the thickness is increased from 15nm to 95nm. The optimum EL signal thus results from a trade-off between layer conductivity (i.e. number of Si-ncs) and Er^{3+} excitation, as drawn on the inset to Fig. 6, both parameters being governed by the excess Si content and layer thickness.

5. Impact of structural factors on external quantum efficiency

To reinforce this study of the structural factors influencing the behavior of the devices, we can estimate the external quantum efficiency (EQE) which represents the number of emitted photons per injected electron Eq. (3):

$$EQE = \frac{n_{\substack{emitted\\photons}}}{n_{\substack{injected\\electrons}}} = A \cdot \left(\frac{e}{h\nu} \cdot \frac{I_{EL}}{I_{injection}} \right) \qquad (3)$$

where I_{EL} is the EL intensity detected around 1.5µm, h is Planck's constant, ν is the frequency of emission, $I_{injection}$ is the injected current and e is the elementary charge on the electron. In the geometry of the setup, only a fraction of the emitted photons is effectively collected by the detection system, and the term A is thus a correction factor that takes into account the collection geometry. For an absolute calculation of the EQE, all emitted photons emitted should be included (i.e. including photons emitted in the visible range). However, as this work aims at optimizing EQE at 1.5 µm, we only calculate the 1.5µm EQE, which represents the number of "useful" photons emitted per injected electron. The resulting values given here are therefore lower than the total EQE.

#167472 - $15.00 USD Received 27 Apr 2012; revised 6 Jul 2012; accepted 12 Jul 2012; published 17 Sep 2012

The evolution of EQE with layer thickness for both values of Si excess (7 and 18 at.%) is shown in Fig. 7. For 7 at.% of Si excess, the value of EQE increases from 0.005% at 20 nm to > 0.2% at 170 nm, i.e. a 40-fold enhancement, whereas for 18 at.% an optimum EQE of about 0.02% is reached around 30-40 nm, but it falls below $10^{-3\%}$ for thinner and thicker samples.

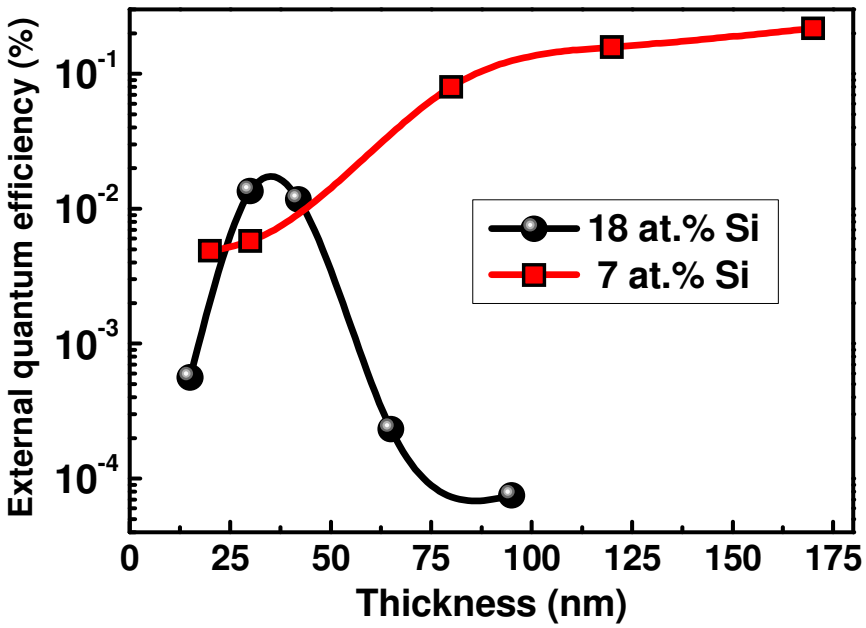

Fig. 7. External quantum efficiency for different thicknesses of SiO_x:Er LEDs containing 7 at.% and 18 at.% excess Si.

The values of EQE are thus not uniquely governed by the thickness, but are also dependent on the excess Si content. The key parameter lies in the degree of agglomeration of excess Si, inasmuch as it plays a major role for both the transport of carriers and the sensitization of Er^{3+}. Such an agglomeration can be tailored by varying both Si excess [31] and thickness [28]. In this view, the rapid increase of EQE during the first stage of thickness increase (from 20 nm to ~100 nm) for 7 at% reflects the enhanced formation of Si-ncs sensitizers. On the other hand, the highest value of EQE is surprisingly achieved at 170 nm, for which the EL signal is low (cf. Fig. 5) and the current density is the lowest (Fig. 2(b) and Fig. 3). The obtained relatively high EQE value (about 0.2%) reflects efficient sensitization of Er^{3+} ions. Thus, even if there are fewer electrons injected in this 'thick' active layer (low conductivity), a sizeable fraction of them is effectively 'useful' for impact excitation of Er^{3+} ions. This is a further indication that generation of hot electrons yields to more efficient excitation of Er^{3+} ions. Besides, for this thick layer and annealing conditions, almost all Si-excess atoms are agglomerated within well-defined Si-ncs [28,31] separated with regions of stoichiometric SiO_2, hence avoiding any scattering from defects in the electron path toward Er^{3+} ions. The resulting low EL, despite the good sensitization of Er^{3+} ions, is the direct consequence of the low current density. Concerning the higher Si excess, the corresponding layers show an optimum EQE at 30-40nm thickness, for which an optimum density of Si-based sensitizers is formed within the active layer. For higher values of the thickness, the high

#167472 - $15.00 USD Received 27 Apr 2012; revised 6 Jul 2012; accepted 12 Jul 2012; published 17 Sep 2012

Si excess is detrimental to the sensitization of Er^{3+} ions probably because of the creation of too much defects and scattering centers.

By comparing the EQE values obtained for low (7 at.%) and high (18 at.%) Si excess at a thickness of 30-40 nm, we noticed a two-fold enhancement of EQE when more sensitizers are formed (18 at.%). However, this better EQE obtained at 30-40 nm for high Si excess is still one order of magnitude lower than the best EQE obtained for thicker sample (170 nm) containing less Si excess. Such a phenomenon is likely to be due to the fact that, even for a high Si excess, the compressive stress still inhibits the agglomeration of Si atoms in thin films, thus not all Si atoms are agglomerated. The resulting isolated Si atoms or structural defects may act as scattering centers that reduce the overall efficiency of sensitization of Er^{3+} ions. This is another indication that relatively large Si-ncs (with trap depth sufficient to create hot electrons) with surrounding near-stoichiometric oxide are needed to ensure efficient excitation of Er^{3+} ions. Such results show that, to increase EQE in SiO_x:Er system, one has to ensure formation of well-defined Si-ncs in perfectly stoichiometric SiO_2. A promising way to obtain that ideal system would be to separate Si-ncs containing layer (SiO_x) from the Er-containing layer (Er:SiO_2) in multiple stacks of monolayers, similar to SiO_x/SiO_2 multilayers recently studied [35,42,43].

Conclusion

We have presented a study that contributes to further understanding of both the electrical transport of carriers mediated by Si-ncs and the process of erbium sensitization by excess silicon in the case of electrical excitation. Such processes have been much less studied in this material than is the case for optical excitation, and yet a proper understanding of carrier transport and sensitization is required not only for a fuller description of the physics of the material, but also as a prerequisite to the development of electrically pumped devices. The picture we reveal is a complex one that highlights the competing effects of stress and excess silicon content in modulating sample conductivity and sensitization efficiency. Our results suggest that the mechanism of carrier transport in SiO_x films depends critically on the distribution of excess silicon. In the case of well-defined silicon nanoclusters separated by regions of stoichiometric or near-stoichiometric oxide, whilst the nanoclusters are efficient sensitizers of erbium emission, the overall conductivity of the sample is low. In contrast, in films in which the excess silicon is distributed across a large number of much smaller silicon nanoinclusions in a largely sub-oxide matrix, film conductivity is much higher, but excitation of erbium ions is very inefficient due to the lack of sensitizing nanoclusters. We propose a model in which hot electron injection into the erbium-containing oxide or suboxide matrix is facilitated by the presence of discrete silicon nanoclusters separated by stoichiometric or near-stoichiometric oxide. However, when the excess silicon in the matrix is more homogeneously distributed, the depth of the silicon-related traps is insufficient to allow for hot electron injection thanks to a decrease in the conduction band offset between the silicon nanoinclusions and the now more silicon-rich suboxide matrix. It is this hot electron injection that is responsible for impact excitation of erbium ions within the oxide, and hence larger well-defined silicon clusters are more efficient at generating erbium luminescence. This model is consistent with the observation that the electrically excitable fraction of erbium in SiOx is higher than the corresponding optically excited number – different populations of erbium ions are being excited in the two cases: in the latter it is only the small number of erbium ions that lie sufficiently close to the silicon nanoclusters for efficient excitation transfer. Our study thus suggests that the interface between silicon-rich and stoichiometric regions (or between Si nanoclusters and SiO_2) plays a vital role in both the carrier transport and sensitization mechanisms. This has important implications, not only for the design of LEDs, lasers and optical amplifiers exploiting these materials, but also for other technologically important systems incorporating semiconductor nanoclusters, such as photovoltaics, in which efficient extraction of carriers is required.

#167472 - $15.00 USD Received 27 Apr 2012; revised 6 Jul 2012; accepted 12 Jul 2012; published 17 Sep 2012